High-energy, shock-front-assisted resonant radiation in the normal dispersion regime

PHYSICAL REVIEW A **88**, 051801(R) (2013)

High-energy, shock-front-assisted resonant radiation in the normal dispersion regime

Thomas Roger,[1] Mohammed F. Saleh,[2] Samudra Roy,[2] Fabio Biancalana,[1,2] Chunyong Li,[1] and Daniele Faccio[1]
[1]*School of Engineering and Physical Sciences, Heriot-Watt University, EH14 4AS Edinburgh, United Kingdom*
[2]*Max Planck Institute for the Science of Light, Günther-Scharowsky strasse 1, 91058 Erlangen, Germany*
(Received 6 May 2013; published 5 November 2013)

We present a simple yet effective theory that predicts the existence of resonant radiation bands in the deep normal group-velocity dispersion region of a medium, even in the absence of a zero-group-velocity dispersion point. This radiation is evident when the medium is pumped with high-energy ultrashort pulses, and it is driven by the interplay between the Kerr and the shock terms in the nonlinear Schrödinger equation. Accurate experiments performed in bulk silica fully support the theoretical phase-matching condition found by our theory.

DOI: 10.1103/PhysRevA.88.051801 PACS number(s): 42.65.Tg, 42.65.Jx, 42.65.Sf

In nonlinear optics, temporal solitons usually propagate in a medium with additional perturbations (such as the Raman effect, higher-order dispersions, external potentials, etc.) and, when the momentum of the soliton matches the propagation constant of the waveguide itself, may emit a kind of radiation known as *resonant radiation* (RR) [1–3]. This *phase matching* typically occurs only for specific frequencies, that can be well separated from the central frequency of the soliton, allowing a powerful energy transfer from the soliton to the radiation.

There has been a recent surge of interest in the phenomenon leading to the formation of resonant radiation in fibers and bulk media. In recent experiments, ultraviolet resonant radiation emitted by blueshifting solitons in hollow-core photonic crystal fibers has been demonstrated [4]. Moreover, resonant radiation has been demonstrated to be responsible, among other mechanisms, for supercontinuum generation in optical fibers and, in particular, in photonic crystal fibers [1–3,5]. Resonant radiation can also be observed in micron-size integrated waveguides [6], in silicon-on-insulator waveguides [7], and even in waveguide arrays where it is emitted by spatial solitons [8]. In hydrodynamics, shallow water solitons can also emit linear waves [9]. This universality has also led to fresh interpretations in the basic processes leading to the formation and control of resonant radiation in optics [10,11].

In previous papers on the subject, it was argued that, in order to generate dispersive resonant radiation, one does not strictly need a soliton since the radiation can be emitted even when pumping in the normal dispersion regime in the presence of a zero-group-velocity dispersion (GVD) point that is sufficiently close to the pump wavelength [12,13]. The phase-matching condition between the pulse and the radiation is essentially identical to the soliton case [13]. All these papers assume the impossibility of creating dispersive waves in the absence of higher-order dispersion (HOD) terms since these traditionally are the sources of the perturbation needed to excite the radiation modes [1–3].

In this Rapid Communication, we show that, when operating in the normal dispersion regime of a medium, it is not necessary to have higher-order dispersion or a zero-GVD point to produce a powerful source of resonant radiation that is well separated from the pump. We have found, rather surprisingly, that only the Kerr effect is needed and that the phase-matching condition is influenced strongly by a previously overlooked effect, namely, shock-front-induced dispersion. We derive a resonant radiation phase-matching condition, and we support our theory with numerical simulations. Moreover, we demonstrate experimentally the existence of the new shock-front-induced resonant radiation by using pulses propagating in normal GVD in bulk silica.

Phase-matching condition for resonant radiation in normal GVD. Propagation of intense ultrashort pulses in a nonlinear medium is described by the following generalized nonlinear Schrödinger equation:

$$i\,\partial_z A + \hat{D}(i\partial_t)A + [1 + \hat{S}(i\partial_t)]\gamma|A|^2 A = 0, \tag{1}$$

where z and t are the longitudinal spatial and temporal coordinates, respectively, $A(z,t)$ is the electric-field envelope, $\hat{D}(i\partial_t) \equiv \sum_{m=2}^{\infty} \beta_m (i\partial_t)^2/m!$ is the dispersion operator, $\hat{S}(i\partial_t) \equiv (i/\omega_0)\partial_t$ is the shock operator, β_m is the mth-order dispersion coefficient, γ is the nonlinear coefficient of the medium, and ω_0 is the central input pulse frequency.

Resonant radiation will be emitted at frequencies for which the propagation constant of the medium matches the input pulse momentum, whether the pulse is a soliton or not. This condition can easily be found by equating the total phase of the pump (ϕ_0) and the total phase of the radiation (ϕ_R) after a common delay $t \equiv z/v_g(\omega_0)$ with $v_g \equiv \beta_1(\omega_0)^{-1}$, where $\beta(\omega)$ is the propagation constant of the medium,

$$\phi_0 = \left\{\beta(\omega_0) - \omega_0/v_g(\omega_0) + \gamma P\left[1 + \frac{\omega - \omega_0}{\omega_0}\right]\right\} z, \tag{2}$$

$$\phi_R = \{\beta(\omega_R) - \omega_R/v_g(\omega_0)\} z. \tag{3}$$

The third term inside the curly brackets in Eq. (2) is due to the combined action of the self-phase modulation (SPM) and the shock operator. The latter is traditionally neglected in the literature since it is supposed to modify the resonant condition only slightly, but in this Rapid Communication, we show that it plays a crucial role in the absence of a zero-GVD point in the vicinity of the pump frequency ω_0. We note that RR is typically emitted with a very different group velocity with respect to the pump pulse so that no cross-phase modulation effects occur: They are, therefore, neglected in (3). The phase-matching condition for the radiation emission, namely, $\phi_0 = \phi_R$, results in the following equation for the frequency detuning $\Delta\omega \equiv \omega_R - \omega_0$ between pulse and radiation, obtained by expanding, in Taylor series, the propagation constant of the radiation

around ω_0:

$$\sum_{m=2}^{\infty} \frac{1}{m!}\beta_m \Delta\omega^m = \gamma P\left[1+\frac{\Delta\omega}{\omega_0}\right]. \tag{4}$$

If only the second-order dispersion coefficient (β_2) is taken into account on the left-hand side of Eq. (4), one obtains the following two resonant radiation frequencies in physical units:

$$\Delta\omega_{\pm} = \frac{\gamma P \pm \sqrt{(\gamma P)^2 + 2\beta_2 \gamma P \omega_0^2}}{\omega_0 \beta_2}. \tag{5}$$

The first solution $\Delta\omega_+$ is always positive, and thus, the resonant radiation associated with this solution is always blueshifted with respect to the pump frequency. The second solution $\Delta\omega_-$ is always negative and close to zero so that the radiation associated with it is always redshifted and very close to the pump frequency and, for this reason, may be rather difficult to observe experimentally. An important and surprising point is that it is not necessary to have a zero-GVD point in the dispersion in order for pulses to emit resonant radiation. The Kerr effect alone, when combined with the pulse propagating in the normal GVD regime of the medium, is sufficient to produce such radiation, which will appear as two identical peaks, spectrally symmetric with respect to the pump. Note that SPM, when combined with the normal GVD, induces the formation of lateral peaks known as "optical-wave breaking" [14], which were noted both experimentally and numerically, and are attributed to four-wave mixing [14,15]. However, the radiation described in this Rapid Communication is of a different nature and has been overlooked in previous studies and recent papers on the subject [12,13] and should be distinguished from optical-wave breaking since it leads to asymmetric relatively far-detuned spectral peaks. However, we note that, recently, self-steepening effects have been considered with respect to the phase-matching condition for spatiotemporal modulational instability gain [16], although not in terms of solitonic propagation.

We first note that, if the shock term and HOD are neglected, then Eq. (5) leads to

$$\Delta\omega_{\pm} \simeq \pm\sqrt{2\gamma P/\beta_2}. \tag{6}$$

In view of the existing literature on resonant radiation from solitons, this result is interesting and is totally unexpected: One does not need HOD or a zero-GVD frequency point in order to observe resonant radiation, but just β_2 and Kerr are necessary in the normal GVD for *sufficiently high laser-pulse powers*. The remaining terms in Eq. (5) indicate that the presence of the shock term and HOD terms can then strongly unbalance the spectral location of the two resonant radiation peaks, which will shift to one side of the spectrum, making one of them (typically the blueshifted one) very visible both numerically and experimentally while hiding the other inside the central spectral body of the input pulse.

Numerical simulations. We now prove the validity of the phase-matching condition Eq. (4) by means of numerical simulations. First of all, we write Eq. (4) in dimensionless units by using the rescaled dimensionless variables $\xi \equiv z/z_0$, $\tau \equiv t/t_0$, $\psi \equiv A/\sqrt{P_0}$, $z_0 \equiv t_0^2/|\beta_2|$, $P_0 \equiv (\gamma z_0)^{-1}$, $\mu_{\rm sh} \equiv (\omega_0 t_0)^{-1}$, $\alpha_m \equiv \beta_m/[|\beta_2| m! t_0^{m-2}]$ ($m \geqslant 3$), and

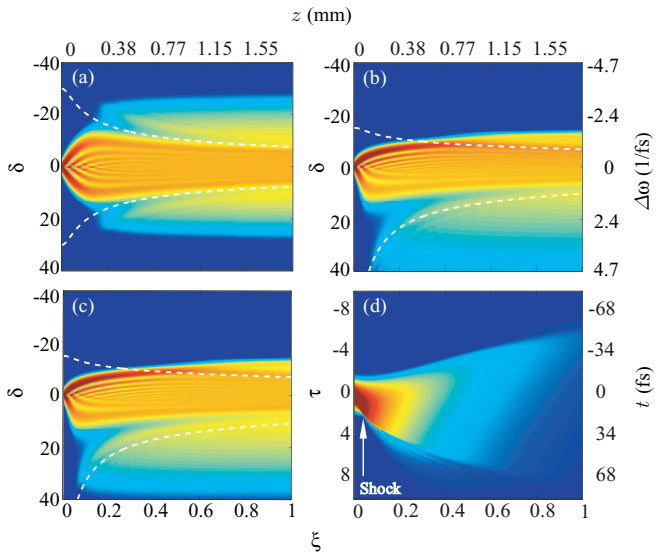

FIG. 1. (Color online) (a) Propagation of an input pulse $\psi_{\rm in} = N\,\mathrm{sech}(\tau)$ in the normal dispersion with $N = 15$, $\alpha_3 = \mu_{\rm sh} = 0$ for one dispersion length $\xi = 1$. (b) Same as (a) but with $\mu_{\rm sh} = 0.05$. (c) Same as (a) but with $\tau = 0.05$ and $\alpha_3 = 0.005$. (d) Contour plot of the pulse propagation in the time domain with the same parameters as in (c). Note that the formation of a shock at $\xi \sim 0.02$ coincides with the moment of the formation of the two spectral sidebands in (c). The dashed white lines denote the position of the RR calculated by using the phase-matching condition Eq. (7). (a)–(d) are plotted in logarithmic scale over 2.5 decades. The white arrow in (d) indicates the point of shock formation.

$\delta \equiv \Delta\omega\, t_0$. The positions of the resonant radiation frequencies Eqs. (5) and (6) in dimensionless units then become

$$\sum_{m\geqslant 2} \alpha_m \delta^m = N^2[1+\mu_{\rm sh}\delta], \tag{7}$$

$$\delta_{\pm} \simeq \pm\sqrt{2}N, \tag{8}$$

$$\delta_{\pm} = N^2\mu_{\rm sh} \pm \sqrt{(N^2\mu_{\rm sh})^2 + 2N^2}. \tag{9}$$

With the above scalings, we then solve Eq. (1) in its dimensionless form by means of a standard split-step Fourier scheme in which the nonlinear part is integrated by means of a fourth-order Runge-Kutta algorithm. We use an input pulse $\psi_{\rm in} = N\,\mathrm{sech}(\tau)$. The results are shown in the panel of Fig. 1. In Fig. 1(a), we show the spectral evolution of a strong pulse of dimensionless amplitude $N = 15$, propagated for $\xi = 1$ (i.e., one second-order dispersion length) in the normal dispersion regime with no higher-order dispersive terms and when neglecting the shock operator, i.e., $\mu_{\rm sh} = 0$. After the usual SPM phase, which broadens the spectrum symmetrically, one can notice around $\xi \sim 0.02$, two sidebands that correspond exactly to the resonant radiation bands described by Eq. (8) (shown by white dashed lines). In this case, only the normal GVD and the Kerr nonlinearity are present, and the two sidebands are perfectly symmetric with respect to $\delta = 0$, i.e., the input pulse frequency. This case is conceptually important but unrealistic since the shock term can never be switched off in practice and constant GVD is very difficult if not impossible to achieve in ordinary waveguides or in bulk media.

In Fig. 1(b), we still do not introduce any higher-order dispersion term, but we introduce a shock term coefficient $\mu_{sh} = 0.05$. Such a value of μ_{sh} would correspond, in dimensional units, to a pulse duration of $t_0 \simeq 8.5$ fs if the pump wavelength is $\lambda_0 \simeq 0.8\ \mu$m. All other parameters are the same as in Fig. 1(a). One can see that introducing the shock term strongly modifies the position of the sidebands, the positions of which become strongly unbalanced with respect to $\delta = 0$. This is also accurately predicted by Eq. (9), represented with white dashed lines in the figure. As discussed above, one of the sidebands shifts its position very close to the input pulse frequency, and is "hidden" inside the spectral body of the self-modulated pulse. The second blueshifted sideband is much more evident and possesses a much broader bandwidth than the redshifted band.

Figure 1(c) is the same as Fig. 1(b) but with an additional third-order dispersion term $\alpha_3 = 0.005$ included. It is evident that third-order dispersion does not dramatically affect the position of the sidebands from the previous cases. More complicated cases, when both the full dispersion and the shock term are included, can easily be studied by solving the generally large polynomial equation Eq. (7). In Fig. 1(d), we show the space-time contour plot of the propagation relative to Fig. 1(c). One can see that the moment when the sidebands start to be emitted spectrally is exactly when a shock appears in the time domain, indicated with an arrow in Fig. 1(d).

Experiments in bulk fused silica glass. A remarkable feature of RR is that it can also be accurately described within the framework of a first Born approximation, i.e., it is essentially a linear-wave scattering process from a time-dependent (moving at speed v) scatterer [17]. Moreover, this has been shown to be true not only in one-dimensional (1D), but also in two-dimensional [18] and three-dimensional (3D) bulk interaction geometries [19,20]. In the full 3D geometry, the standard momentum relation for RR in the 1D case becomes a relation for the (propagation direction) z component of the 3D wave vector, which, accounting for the shock term introduced in Eq. (5), reads as

$$k_z(\omega) = k(\omega_0) + \frac{(\omega - \omega_0)}{v} - \gamma P \frac{\Delta\omega}{\omega_0}. \tag{10}$$

The full (θ,λ) location of the 3D RR peak is then given by $\theta \sim k_\perp/k = \sqrt{1-(k_z/k)^2}$, where $k = \omega n(\omega)/c$. Experiments may, therefore, be either carried out in 1D fiber geometries or, more conveniently from the perspective of attaining high pulse intensities, in a 3D bulk geometry. Following this idea, we carried out experiments in bulk fused silica glass. We used an input Bessel pulse in order to achieve the essential conditions required for observing shock-front-induced RR: (i) The nondiffracting Bessel peak gives an effective fiberlike propagation regime with sustained peak intensities over long distances, (ii) the spatial Bessel dynamics lead to an effective suppression of transverse spatial instabilities, in particular, self-focusing and filamentation that typically dominate Gaussian pulse propagation [21], (iii) high intensities (multi-TW/cm^2) are attained due to the suppression of filamentation effects, i.e., suppression of the clamping of the peak intensity to a maximum value that typically occurs with Gaussian pulses [21].

In our experiments, ultrashort optical pulses ($t_0 \sim 100$ fs, central wavelength 785 nm) are shaped into Bessel beams using an axicon of base angle $\theta = 3^\circ$ that creates an intense on-axis central peak ($I_{max} = 8$ TW/cm^2). This intense peak is normally incident onto a $\sim$1.5-cm-thick piece of fused silica.

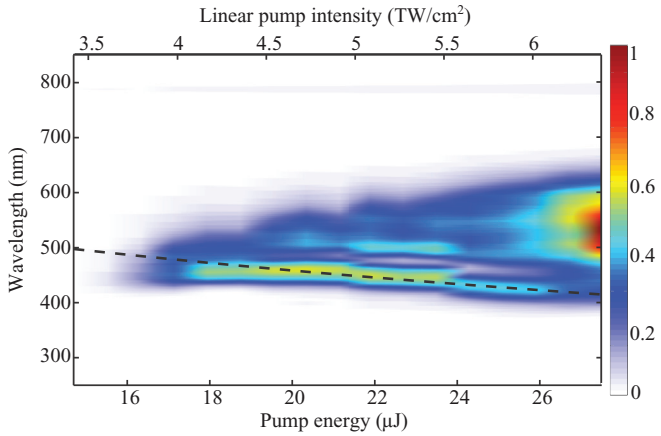

FIG. 2. (Color online) Evolution of spectral broadening from a Bessel beam in bulk fused silica as the intensity of the beam is increased. The lower x axis shows the average energy of the pulses, whereas, the upper x axis estimates the peak intensity of the Bessel beam at the position of the fused silica block. The spectra were measured after a filter that has a sharp long-wavelength cutoff for $\lambda > 700$ nm. The input pump pulse spectrum, therefore, only appears as a very weak feature at 785 nm. The dashed line shows the fit of Eq. (11), which fits well over the range of energies used in this study.

In Fig. 2, we show the output spectra measured with a fiber spectrometer (Ocean Optics HD4000), integrated over the width of the beam. A filter that cuts all wavelengths above 700–750 nm is included in order to avoid saturation and damage from the pump beam. The input pump energy is increased ranging from 15 to 27 μJ corresponding, for the Bessel angle and wavelength used here, to intensities ranging from 3.5 to 6.5 TW/cm^2 (indicated in the figure). At low input energies (15–18 μJ), there is spectral broadening generated by SPM from the input pulse. For higher input energies, we observe the formation of a separated peak at a wavelength that blueshifts with increasing pump energy. At higher input energies ($>26\ \mu$J), filamentation dynamics finally take over, and supercontinuum generation washes out the separated peak around 400 nm. We interpret the isolated blue spectral peak (for energies $<26\ \mu$J) as evidence for shock-induced resonant radiation. Indeed, we fit this peak using Eq. (5) after a Taylor expansion to second order, this providing an equation for the wavelength of the RR,

$$\lambda_{RR} = \frac{\lambda_0}{1 + x + \sqrt{x(2+x)}}$$

where

$$x = \frac{n_2 I k_0 \lambda_0^2}{2\pi^2 c^2 |\beta_2|}. \tag{11}$$

Here $n_2 = 3 \times 10^{-16}$ cm^2/W [22] is the nonlinear refractive index of the fused silica, and the second-order dispersion coefficient is $\beta_2 = 3.7 \times 10^{-26}$ s^2/m [15], whereas, the peak intensity is calculated using the standard equation for linear Bessel beam propagation [see Supplemental Material [23], Eq. (1)].

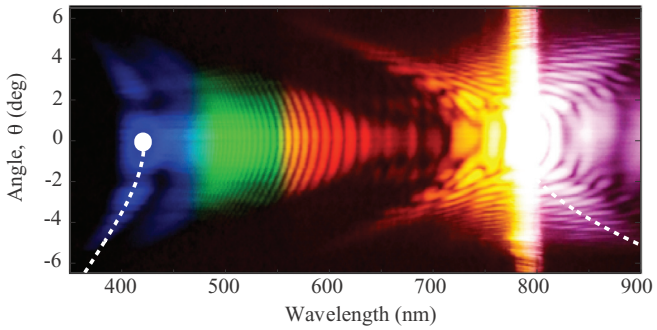

FIG. 3. (Color online) Measured spectrum at a pump intensity of $\sim$21 μJ following the formation of the shock front, which induces the RR described by Eq. (5). Dashed white line: fit from Eq. (10). Solid white circle: 1D solution from Eq. (5).

This approximation is valid for all input energies below the filamentation threshold ($E_{\text{in}} \lesssim 25$ μJ), i.e., below the threshold for which nonlinear beam reshaping dynamics take over and completely dominate the pulse evolution. We underline that, when fitting with this equation, there are no free parameters, yet as shown by the dashed black line in Fig. 2, we obtain an excellent fit to the experimental data. In the Supplemental Material [23], we compare measurements for the Bessel pulse (shown in Fig. 2) with an input Gaussian pulse. The Gaussian pulse shows evident filamentation dynamics and supercontinuum generation for input peak intensities that are more than one order of magnitude lower than the observed Bessel beam filamentation threshold. Therefore, with a Gaussian beam, the shock-induced RR is either simply not excited (due to the lower peak intensities) or may still be present but, in any case, is covered by the filament supercontinuum and is not distinguishable as a separate peak. Conversely, with Bessel beam filamentation, supercontinuum occurs only at much higher intensities. We note that our experiments in bulk media allow us to measure the full space-time spectra in (θ,λ) coordinates [20,24,25].

In Fig. 3, we show the far-field (θ,λ) spectrum for a pump energy of $\sim$21 μJ. This spectrum is measured using a homebuilt imaging spectrometer and a modified digital camera. The latter allows measurement of spectra without the need for any additional filters to cut the pump beam, thus, the whole frequency spectrum is now clearly visible. Figure 3 shows a clear blueshifted peak close to 400 nm that is separated from the rest of the spectrum and whose position and shape are well reproduced by Eq. (10) (dashed white line) where the peak intensity is taken as the intensity at the sample input facet (see Supplemental Material [23]). The full white circle in the figure shows the calculated wavelength for shock-induced resonant radiation as predicted by the $\Delta\omega_+$ solution to the 1D relation Eq. (5). This solution naturally coincides with the full 3D fit for $\theta = 0^\circ$. The full far-field evolution (for increasing input energy) of the spectral broadening is shown in the Supplemental Material [23].

Conclusions. We have demonstrated, theoretically and experimentally, a form of resonant radiation that is solely is the result of the high laser pulse intensity and is highly visible in the presence of a shock front in the form of a blueshifted spectral peak. This form of wave breaking finds a quantitative description in terms of a generalized linear-wave resonant scattering process that occurs in normal GVD and even in the absence of a zero-GVD point. The ubiquity of similar shock-front dynamics in other systems, e.g., gravity waves in water or in plasma waves, points to similar wave scattering processes that should also appear in the same form as described here. The ability to control such radiation can lead to novel ways to implement and to control the generation of supercontinua which are modulationally stable and with higher coherence. Likewise, at the quantum level, recently discovered vacuum squeezing associated with RR [26] may benefit from generation when starting from a stable background state.

Acknowledgments. D.F. acknowledges financial support from the Engineering and Physical Sciences Research Council EPSRC, Grant No. EP/J00443X/1 and from the European Research Council under the European Union's Seventh Framework Programme (Grant No. FP/2007-2013)/ERC Grant Agreement No. 306559.

[1] A. V. Husakou and J. Herrmann, Phys. Rev. Lett. **87**, 203901 (2001).
[2] N. Akhmediev and M. Karlsson, Phys. Rev. A **51**, 2602 (1995).
[3] F. Biancalana, D. V. Skryabin, and A. V. Yulin, Phys. Rev. E **70**, 016615 (2004).
[4] N. Y. Joly *et al*., Phys. Rev. Lett. **106**, 203901 (2011).
[5] J. M. Dudley *et al*., Rev. Mod. Phys. **78**, 1135 (2006).
[6] P. Colman, S. Combrié, G. Lehoucq, A. de Rossi, and S. Trillo, Phys. Rev. Lett. **109**, 093901 (2012).
[7] W. Ding *et al*., Opt. Express **18**, 26625 (2010).
[8] Tr. X. Tran and F. Biancalana, Phys. Rev. Lett. **110**, 113903 (2013).
[9] V. I. Karpman, Phys. Rev. E **58**, 5070 (1998).
[10] M. Erkintalo, Y. Q. Xu, S. G. Murdoch, J. M. Dudley, and G. Genty, Phys. Rev. Lett. **109**, 223904 (2012).
[11] E. Rubino, J. McLenaghan, S. C. Kehr, F. Belgiorno, D. Townsend, S. Rohr, C. E. Kuklewicz, U. Leonhardt, F. Konig, and D. Faccio, Phys. Rev. Lett. **108**, 253901 (2012)
[12] S. Roy *et al*., Opt. Commun. **283**, 3081 (2010); Appl. Opt. **50**, 3475 (2011).
[13] K. E. Webb *et al*., Opt. Lett. **38**, 151 (2013).
[14] W. J. Tomlison, R. H. Stolen, and A. M. Johnson, Opt. Lett. **10**, 457 (1985). See also Ref. [15], pp. 94–97.
[15] G. P. Agrawal, *Nonlinear Fiber Optics*, 4th ed. (Academic, San Diego, 2006).
[16] P. Bejot, B. Kibler, E. Hertz, B. Lavorel, and O. Faucher, Phys. Rev. A **83**, 013830 (2011).
[17] M. Kolesik, L. Tartara, and J. V. Moloney, Phys. Rev. A **82**, 045802 (2010).
[18] M. Kolesik, D. Faccio, E. M. Wright, P. Di Trapani, and J. V. Moloney, Opt. Lett. **34**, 286 (2009).
[19] M. Kolesik, E. M. Wright, and J. V. Moloney, Opt. Express **13**, 10729 (2005).
[20] D. Faccio *et al*., Opt. Express **15**, 13077 (2007).
[21] D. Faccio *et al*., Phys. Rev. A **85**, 033829 (2012).

[22] R. W. Boyd, *Nonlinear Optics*, 2nd ed. (Academic, San Diego, 2003).

[23] See Supplemental Material at http://link.aps.org/supplemental/10.1103/PhysRevA.88.051801 for experimental layout, comparison of input Gaussian and Bessel pulses and calculation of Bessel intensity within the sample.

[24] M. Kolesik, E. M. Wright, and J. V. Moloney, Phys. Rev. Lett. **92**, 253901 (2004).

[25] D. Faccio, M. A. Porras, A. Dubietis, F. Bragheri, A. Couairon, and P. Di Trapani, Phys. Rev. Lett. **96**, 193901 (2006).

[26] T. X. Tran, K. N. Cassemiro, C. Söller, K. J. Blow, and F. Biancalana, Phys. Rev. A **84**, 013824 (2011)